RRB-87-70

SATELLITE OBSERVATIONS OF SEDIMENT TRANSPORT PATTERNS IN THE LAC SAINT-PIERRE REGION OF THE ST. LAWRENCE RIVER

by

J.E. Bruton, J.H. Jerome
and R.P. Bukata

Rivers Research Branch
National Water Research Institute
Canada Centre for Inland Waters
Burlington, Ontario, Canada L7R 4A6

NWRI Contribution #88-87

ABSTRACT

Satellite data from Landsats 4 and 5 were utilized to delineate the seasonal variations of sediment transport zones in the Lac Saint-Pierre region of the St. Lawrence River corridor. A seasonally cyclic succession of patterns displaying persistent, mutually independent, and extensive (in both space and time) turbidity zones was clearly in evidence. Visible and thermal data in both imagery and digital formats were used to show the close relationships existing among the distinct zonal synoptic patterns, the bathymetry of lake and river, and the near surface aquatic temperatures.

RÉSUMÉ

Des données provenant des satellites LANDSAT 4 et 5 ont servi à délimiter les variations saisonnières des zones de transport des sédiments dans la région du lac St-Pierre du corridor du fleuve St-Laurent. Une succession cyclique de configurations saisonnières présentant des zones de turbidité persistantes, indépendantes les unes des autres et étendues (dans le temps et l'espace) est apparue clairement. Des données dans les bandes visibles et thermiques sous forme d'imagerie et d'ensembles numériques ont servi à montrer les rapports étroits existants entre les diverses configurations synoptiques zonales, la bathymétrie du lac et du fleuve et les températures de l'eau près de la surface.

MANAGEMENT PERSPECTIVE

Monitoring the toxic status and modelling the behavioural response of the St.Lawrence River aquatic ecosystem corridor are certainly important concerns of NWRI. Both *in situ* monitoring and theoretical model development are dependent upon an effective and reliable sampling strategy. This manuscript attempts to assist the development of such sampling strategies by utilizing satellite overviews of the St. Lawrence river to illustrate the cyclic seasonal patterns that persistently define the flow-through system. Landsat data (both in imagery format and digital tape format for use on the NWRI DADS system) are used to delineate the extended regions of temporally persistent, mutually independent turbidity zones, their seasonal cycle, and their associations with both bottom topography and near-surface temperature.

PERSPECTIVE GESTION

La surveillance de la toxicité et la modélisation du comportement du corridor de l'écosystème aquatique du fleuve St-Laurent sont certainement des préoccupations de l'INRE. La surveillance in situ et l'élaboration de modèles théoriques dépendent d'une stratégie d'échantillonnage efficace et fiable. La présente étude vise à aider à l'élaboration de telles stratégies d'échantillonnage par l'utilisation d'images satellitaires du St-Laurent afin d'illustrer les configurations saisonnières cycliques qui définissent en tout temps le système d'écoulement. Des données Landsat (sous forme d'imagerie et en bandes numériques exploitées dans le système DADS de l'INRE) servent à délimiter les importantes zones de turbidité, indépendantes les unes des autres et persistantes dans le temps et à déterminer leurs cycles saisonniers et leur association avec la topographie de fond et la température près de la surface.

INTRODUCTION

The aquatic transport corridor, extending from the Upper Great Lakes through Lake St. Clair and the Lower Great Lakes and eventually evacuating into the Atlantic Ocean through the St. Lawrence River, is directly responsive to all aquatic regimes comprising the extensive Great Lakes Basin. Consequently, the water quality of the St. Lawrence River is vulnerable not only to directly inflicted local abuses, but also more distantly inflicted abuses throughout the Great Lakes network. Since the St. Lawrence River occupies such a prominent position in the North American ecosystem, it is understandable that much scientific research has been and is being focused on the chemical and biological aspects of the St. Lawrence River and its network of interacting channels and riverine lakes (Beland, 1974; Allan, 1986; Sloterdijk, 1984; 1987; Lum and Kaiser, 1986; Rao and Mudroch, 1986; Germain and Janson, 1984; amongst others).

Water quality concerns require reliable in situ measurements of toxic contaminant concentrations, which may be confidently used not only as monitoring parameters, but also as meaningful inputs to predictive environmental models. Obtaining reliable in situ measurements, in turn, is strongly dependent upon a sampling strategy (Ongley, 1986; El-Shaarawi, 1984) that accurately incorporates both the independent and responsive behaviours of the ecosystem being monitored. The development of such a sampling strategy may be greatly assisted by the detailed information available from synoptic overviews

of the monitored area. In an attempt to provide such inputs into future sampling strategies of the Lower Great Lakes/St. Lawrence River contaminant transport and fate studies, this manuscript addresses cyclic and persistent features of aquatic regimes delineated in satellite overviews. Due to the significant cost factors involved in obtaining satellite (in this case Landsat) data, as well as the spatial limitations of each satellite-acquired data frame (~185 km x ~185 km), this current study restricted its focus to the riverine lake Lac Saint-Pierre (the most easterly of the three riverine lakes between Lake Ontario and the St. Lawrence Estuary) and the portion of the St. Lawrence River immediately eastward of Lac Saint-Pierre. Similar studies may be conducted for the other riverine lakes (Lacs Saint-Francois and Saint-Louis) and the more easterly segments of the St. Lawrence River).

Fifteen Landsat scenes of the Lac Saint-Pierre region were obtained in imagery format from the Multispectral Scanner (MSS), which provides an individual pixel (picture scene element) resolution of ~80 m x ~80 m. In addition, one scene of the Lac Saint-Pierre region was obtained in digital magnetic tape format from the Thematic Mapper (TM) for more detailed analyses (individual pixel resolution of ~30 m x ~30 m) on the NWRI Digital Analysis and Display System (DADS).

SYNOPTIC PATTERNS OBSERVED OVER THE LAC SAINT-PIERRE REGION

From an examination of 15 Landsat MSS images obtained in the time frame 1983-1986, four distinct classes of Lac Saint-Pierre/ St. Lawrence River synoptic patterns were observed. These may be described as follows:

PATTERN A

This is essentially a winter months pattern characterized by landfast ice on the southern shoreline of Lac Saint-Pierre, and floating ice/water admixtures along the ship channel and other topographical features of the lake proper. Comparatively little landfast ice is observable along the northern shoreline. This differential in ice formation is probably related to the larger shallow marsh regions associated with the southern shore, coupled with the generally major current flow through the northern half of the lake.

These lake patterns tend to continue eastward from Lac Saint-Pierre along the St. Lawrence River with landfast ice being primarily observed along the generally shallower (compared to the northern shoreline) southern shoreline.

An example of Pattern A is illustrated in Figure 1 which depicts the Landsat 5 MSS Band 2 (0.6 μm - 0.7 μm) image collected over Lac Saint-Pierre/St. Lawrence River on February 28, 1985.

PATTERN B

A series of Landsat images, obtained during April and May, are characterized by the clearest water regimes being located in the centre of Lac Saint-Pierre with the most turbid water regimes being located on the northern and/or southern shorelines.

These aquatic regimes tend to retain their independent identities as they move eastward along the St. Lawrence River towards the Estuary. Lac Saint-Pierre, however, does not generate the independence of the flow-through aquatic regimes (although it does serve to modulate the patterns) since independent aquatic regime behaviour is observable in the St. Lawrence River west of Lac Saint-Pierre. In general, the turbidity regimes along the northern shore appear to possess a higher degree of lateral diffusion (or a less sharp turbidity gradient) than do the more distinctly striated (sharp lateral turbidity gradient) turbidity zones along the southern shore.

Figure 2 illustrates a Pattern B configuration recorded by the Landsat 4 MSS Band 2 (0.6 μm - 0.7 μm) sensor on May 6, 1983.

PATTERN C

This pattern, generally observable in the early summer, is characterized by considerable lateral diffusion (or, alternatively, a relatively flat turbidity gradient for predominantly zoned aquatic

transport). The main body of turbidity appears associated with the centre of Lac Saint-Pierre with lesser concentrations of turbidity apparent on the shores.

It still appears, both in the St. Lawrence River and Lac Saint-Pierre, that the turbidity zones maintain their mutual independence. However, the turbidity gradient from zone to zone has diminished considerably, giving a synoptic observer the impression of zeroth order surficial homogeneity. Whether this drop in lateral turbidity gradient is a consequence of lateral or vertical mixing and/or diffusion would be highly speculative at this stage.

Figure 3 shows a Pattern C configuration recorded by the Landsat 5 MSS Band 2 sensor on June 17, 1984.

PATTERN D

This pattern is the most distinct and also perhaps most stable configuration defining the area of study. It was prominently observed on August 4, 1984, August 20, 1984, and September 16, 1985 in an almost identical overlay pattern. With somewhat less stability, it was appearing to form on the June 23, 1983 image and continued to persist on the October 31, 1984 image. However, it was rapidly deteriorating on the November 8, 1984 image eight days later. Consequently, this principal pattern may be taken, with reasonable confidence, to be the operative pattern from late June to late October.

Pattern D is characterized by distinct turbidity zones, indicating mutually independent (near-zero interaction) aquatic flow-through regimes from the St. Lawrence River through Lac Saint-Pierre and eastward into and along the St. Lawrence River.

Pattern D, however, in contrast to Pattern B, displays its most turbid zones in the centre of the lake and river. The peak concentration of turbidity aligns directly with the principal dredged ship channel. As will be discussed later, the other major turbidity zones are directly aligned with the bathymetry.

Figures 4, 5 and 6 show the Pattern D configurations recorded by the Landsat 5, MSS Band 2 sensor on August 4, 1984, the Landsat 5 MSS Band 2 sensor on August 20, 1984, and the Landsat 4 MSS Band 2 sensor on September 16, 1985, respectively. The almost identical nature of these images is readily apparent, underscoring the longevity of this synoptic pattern.

As mentioned, in addition to the well-defined and easily recognizable patterns A, B, C and D characterizing the Landsat images, there were also several hybrid patterns encountered in the Landsat data considered herein. In particular, hybrid patterns frequently occurred combining features of patterns C and D, i.e., distinct conditions of both strongly striated turbidity transport zones coupled with substantial inter-zonal diffuse patterns.

Table 1 summarizes the dates and patterns observed in the Landsat images considered in this study of the Lac Saint-Pierre/St. Lawrence River region. The dates and patterns of Table 1 strongly suggest the

seasonal cycle schematically shown in Figure 7. The ice pattern A persists through the winter months (November to March). Subsequent to ice melt, Pattern B develops wherein distinct turbidity zones begin to be observed throughout Lac Saint-Pierre and the St. Lawrence River. These turbidity zones tend to align with the bottom depth contours, with the clearest water masses associated with the central zones of the lake and river, and the most turbid water masses associated with the zones nearest the shores. Pattern B appears to be rather short-lived (early spring, April to May) corresponding roughly to the spring run-off period. As run-off subsides, the turbidity zones appear to maintain their independent identities throughout both the river and riverine lake systems. However, a lateral isotropy develops and Pattern C, characterized by diffuse surficial turbidity becomes the prominent pattern from mid May to late June. From late June to late October, the distinct patterns of the turbidity zones re-emerge and the most stable, longest-lived of all the patterns, Pattern D persists. Pattern D, however, is the inverse of Pattern B, in that the highest turbidity is now located in the central zones.

DIGITAL ANALYSIS AND DISPLAY SYSTEM (DADS)

DADS is a microcomputer-based image processing, analysis, and display system located in Rivers Research Branch, NWRI and devoted primarily to the scientific analysis of digital multispectral data collected remotely from environmental satellites. The host computer

for the system is an IBM PC-AT. The display has an addressable resolution of 512 picture elements (pixels) horizontally by 512 lines vertically by 32 bits of data per pixel. Of the 32 bits, 24 are assigned to the three primary colours (eight each to red, green, and blue) with the remaining eight bits available for graphic overlays. The primary application software for DADS is the PCI Inc. EASI/PACE image analysis package.

A virtually cloud-free scene of the Lac Saint-Pierre/St. Lawrence River area was obtained from the Landsat 5 Thematic Mapper sensor for the Pattern D configuration observable on August 20, 1984. The satellite data comprise a seven-vector spectral response covering the wavelength intervals (0.45 μm - 0.52 μm, visible blue), (0.52 μm - 0.60 μm, visible green), (0.63 μm - 0.69 μm, visible red), (0.76 μm - 0.90 μm, near infra-red), (1.55 μm - 1.75 μm, near infra-red), (2.08 μm - 2.35 μm, near infra-red), and (10.4 μm - 12.5 μm, thermal infra-red).

Plate 1(a) illustrates the DADS representation of the Landsat digital radiance data as a true colour composite of the first three spectral bands (visible blue, visible green, and visible red) of the Thematic Mapper. The Pattern D configuration is clearly evident both in the Lac Saint-Pierre and St. Lawrence River segments of the image. An enlarged, higher resolution view of the Lac Saint-Pierre sediment transport zones is shown in Plate 1(b), also as a true colour three-band composite. Clearly evident is the distinct independence of the individual transport zones. Turbidity zones associated with

riverine inputs to Lac Saint-Pierre remain independent of and do not interact strongly with the already established turbidity zones associated with the principal aquatic evacuation routes of the St. Lawrence River system. A further enlarged, increased resolution illustration of this independence of turbidity zones is given in Plate 1(c). The western input network to Lac Saint-Pierre is shown along with the three-band true colour representation of the converging streams of aquatic inputs. The persistent independence of the transport zones with respect to lateral diffusion is clearly apparent. This persistent lateral independence of geographically extended and longitudinally moving turbidity regimes is also a consistent feature of the St. Lawrence River. Plate 1(d) shows an increased resolution true colour DADS representation of the St. Lawrence River eastward from Lac Saint-Pierre. The lateral independence of the turbidity zones, both from one another as well as from those zones associated with external riverine and channel inputs, is clearly evident.

Plate 2 illustrates the DADS representations of the Landsat thermal infra-red equivalents of the scenes of Plate 1. Plate 2(a) is a false colour thermal map of the extended Lac Saint-Pierre/St. Lawrence River region, Plate 2(b) is a false colour thermal map of the increased resolution satellite view of Lac Saint-Pierre, Plate 2(c) is a false colour thermal map of the western input network to Lac Saint-Pierre, and Plate 2(d) is a false colour thermal map of the St. Lawrence River eastward from Lac Saint-Pierre. All the digital data

displayed in Plate 2 were acquired in the (10.4 μm - 12.5 μm) Thematic Mapper band, although with a coarser pixel resolution (120 m x 120 m) than were the visible band data (30 m x 30 m) shown in Plate 1. The Landsat digital thermal band data were converted into surface temperatures using the methodologies described in NASA (1984) and Lathrop and Lillesand (1987). Table 2 lists the results of these methodologies and associates, in descending order of temperatures, the near-surface temperature scales for the false colour images of Plate 2. It must be cautioned, however, that the NASA (1984) temperature scale does not take into account atmospheric contributions to the observed temperatures, and neither of the methodologies adequately compensates for cooling at the air/water interface due to surface evaporation. The thermal maps of Plate 2 can, however, be confidently taken to represent a relative, if not absolute, surficial water temperature amongst the component water masses. Despite these thermal caveats, it is readily seen that the thermal and visible satellite-generated maps (Plates 2 and 1, respectively) display very distinct similarities. Not only are they both Pattern D configurations, but the warmest surficial aquatic temperatures are associated with the highest concentrations of turbidity, while the coolest surficial aquatic temperatures are associated with the lowest concentrations of turbidity.

DISCUSSION

Figure 8 depicts a schematic representation of the bathymetry of Lac Saint-Pierre, illustrating the shallow nature of the St. Lawrence system. Most of the lake is $\leq$ 6 feet in depth with the deepest region of the lake (~30 - 35 ft) being a consequence of the dredged shipping lane. The direct relationships among the visible and thermal patterns (Patterns B, C, and D) and the bottom contour features are evident, with (in the case of Pattern D) the highest concentrations of turbidity being associated with the deepest regions of the Lac Saint-Pierre/St. Lawrence River evacuation route. Pattern B displays the opposite relationship to Pattern D, while Pattern C displays some intermediate relationship. There is evidence, on the basis of the observable synoptic patterns that, while some of the input turbidity zones to Lac Saint-Pierre are capable of faithful alignment with the bathymetry (i.e. are capable of negotiating relatively sharp meanderings of the ship channel), some proceed along alternate, albeit comparable, bathymetric features. An example of this latter situation is evident from Plates 1 and 2 which suggest that both temperature and turbidity attempt a secondary linkage between the relatively deep sections (18-30 foot contours) and the input and output ends of Lac Saint-Pierre. These relationships among sediment concentrations, bottom depth contours, and thermal evolution over a yearly cycle certainly merit further study, as does the persistent independence of the sediment transport zones throughout the main evacuation route of the St. Lawrence River corridor.

It might perhaps be tempting to suggest that the high turbidity zone in the centre of the river and lake (and almost completely aligned with the dredged shipping channel) during the summer is a consequence of bottom stirring and resuspension attributable to ship traffic. Indeed some sediment in the channel may undergo movement as turbulence is induced from ship passage. However, an inordinate continuum of high speed ship traffic over an excessively extended distance and time frame would need to be invoked to render such a suggestion tenable. Further, such ship traffic does not explain the cyclic, seasonal behaviour of the A, B, C, and D synoptic patterns.

Such extended regions of temporally persistent independent turbidity zones are not unique in the environment, and, in fact, are a common occurrence in the Great Lakes system (Duane, 1967; Bukata et al., 1974; Lachance et al, 1979). However, the existence, the persistence, and the possible ephemeral variability of these well-defined and mutually independent turbidity zones must be considered as essential elements in the sampling strategies of studies dedicated to the basic understanding of the fates of materials injected into ecosystems as extensive and complex as those comprising the St. Lawrence River transport corridor.

REFERENCES

Allan, R.J., 1986. The limnological units of the Lower Great Lakes - St. Lawrence River corridor and their role in the source and aquatic fate of toxic contaminants. Water Poll. Res. J. Canada, 21(2): 168-186.

Beland, J., 1974. Étude de la qualité des eaux, fleuve Saint-Laurent, tronçon Varennes-Montmagny, Étude du fleuve Saint-Laurent report, Serv. de Prot. de l'Environ du Qué., Sainte Foy, Qué.: 256 pp.

Bukata, R.P., Haras, W.S., and Bruton, J.E., 1974. Space observations of lake coastal processes in Lake Huron and Lake St. Clair. Proc. Second Can. Symp. on Rem. Sens.: 531-549.

Duane, D.B., 1967. Characteristics of the sediment load in the St. Clair River. Proc. Tenth Conf. on Great Lakes Res.: 115-132.

El-Shaarawi, A.H., 1984. Sampling strategy for future data collection. Chapter 7 of statistical assessment of the Great Lakes Surveillance Program, 1966-1981, Lake Erie. Environ. Can. Scientific Series No. 136: 233-264.

Germain, A. and Janson, M., 1984. Qualité des eaux du fleuve Saint-Laurent de Cornwall à Québec (1977-1981). Environ. Can., direction générale des eaux intérieures, region du Québec: 232 pp.

Lachance, M., Bobee, B., and Gouin, D., 1979. Characterization of the water quality in the St. Lawrence River: determination of homogeneous zones by correspondence analysis. Water Resources Res., 15(6): 1451-1462.

Lathrop, R.G. and Lillesand, T.M., 1987. Calibration of Thematic Mapper thermal data for water surface temperature mapping: case study on the Great Lakes. Rem. Sens. of Environ., 22: 297-307.

Lum., K.R. and Kaiser, K.L.E., 1986. Organic and inorganic contaminants in the St. Lawrence River: some preliminary results on their distribution. Water Poll. Res. J. Canada, 21(4): 592-603.

NASA, 1984. Thematic Mapper design through flight evaluation. Final report, Santa Barbara Research Center, N85-19492: 208 pp.

Ongley, E.D., 1986. Considerations for network design for water quantity and quality surveys in Canada. Water Poll. Res. J. Canada, 21(1): 33-49.

Rao, S.S. and Mudroch, A., 1986. Microbial responses to trace elements and nutrients in St. Lawrence River. Water Poll. Res. J. Canada, 21(4): 513-523.

Sloterdijk, H., 1984. Toxic chemicals in the St. Lawrence River. Conf. of the CAN-AM Chemical Congress, Montreal, June 1984. Unpublished manuscript, 7 pp.

Sloterdijk, H., 1987. Use of young-of-the-year fish as bioindicators of toxic chemicals to complement the water quality network in the St. Lawrence River, Quebec province. Water Quality Monitoring Design, IWD/LD Technical Workshop Series No. 6: 47-67.

TABLE 1. Summary of aquatic patterns observed over Lac Saint-Pierre/St. Lawrence River in Landsat imagery.

Date	Landsat	Pattern	Brief Description
Feb. 28, 1985 Mar. 16, 1985	5 5	A	Ice mainly on south shore of lake and river.
May 6, 1983 Apr. 22, 1984 Apr. 17, 1985 Apr. 25, 1985 Apr. 28, 1986	4 4 5 4 4	B	Independent turbidity zones appear in lake and river - clearest water observed in centre, most turbid along shores.
May 24, 1984 June 17, 1984	4 5	C	Diffuse turbidity-relatively flat lateral turbidity gradient.
Aug. 4, 1984 Aug. 20, 1984 Sep. 16, 1985	5 5 4	D	Very distinct independent turbidity zones in lake and river - clearest water observed along shores, most turbid in centre.
Jun. 23, 1983 Oct. 31, 1984 Nov. 8, 1984	4 4 5	Hybrid C/D	Suggestions of both strongly striated zones and laterally diffuse turbidity

TABLE 2. Temperature scales for the false colour satellite thermal maps shown in Plate 2.

False Colour	Temperature °C NASA (1984)	Temperature °C Lathrop and Lillesand (1987)
Red	18.0	18.2
Orange	17.5	17.7
Yellow	17.1	17.2
Pale Green	16.6	16.8
Light Green	16.1	16.3
Medium Green	15.6	15.8
Dark Green	15.2	15.4
Cyan	14.7	14.9
Light Blue	14.2	14.5
Dark Blue	13.8	14.0

FIGURE CAPTIONS

Figure 1: Example of Pattern A recorded by Landsat 5 on February 28, 1985

Figure 2: Example of Pattern B recorded by Landsat 4 on May 6, 1983.

Figure 3: Example of Pattern C recorded by Landsat 5 on June 17, 1984.

Figure 4: Example of Pattern D recorded by Landsat 5 on August 4, 1984.

Figure 5: Example of Pattern D recorded by Landsat 5 on August 20, 1984.

Figure 6: Example of Pattern D recorded by Landsat 4 on September 16, 1985.

Figure 7: The seasonal cycle of synoptic patterns observable over the Lac Saint-Pierre region of the St. Lawrence River.

Figure 8: The bathymetry contours of Lac Saint-Pierre.

Plate 1(a): DADS true colour composite of Landsat data over Lac Saint-Pierre and the St. Lawrence River observed on August 20, 1984.

Plate 1(b): DADS true colour composite of Landsat data over Lac Saint-Pierre observed on August 20, 1984.

Plate 1(c): DADS true colour composite of Landsat data over the western input network to Lac Saint-Pierre observed on August 20, 1984.

Plate 1(d): DADS true colour composite of Landsat data over the St. Lawrence River observed on August 20, 1984.

Plate 2(a): DADS false colour thermal map of Landsat data over Lac Saint-Pierre and the St. Lawrence River observed on August 20, 1984.

Plate 2(b): DADS false colour thermal map of Landsat data over Lac Saint-Pierre observed on August 20, 1984.

Plate 2(c): DADS false colour thermal map of Landsat data over the western input network to Lac Saint-Pierre observed on August 20, 1984.

Plate 2(d): DADS false colour thermal map of Landsat data over the St. Lawrence River observed on August 20, 1984.

Figure 1

Figure 2

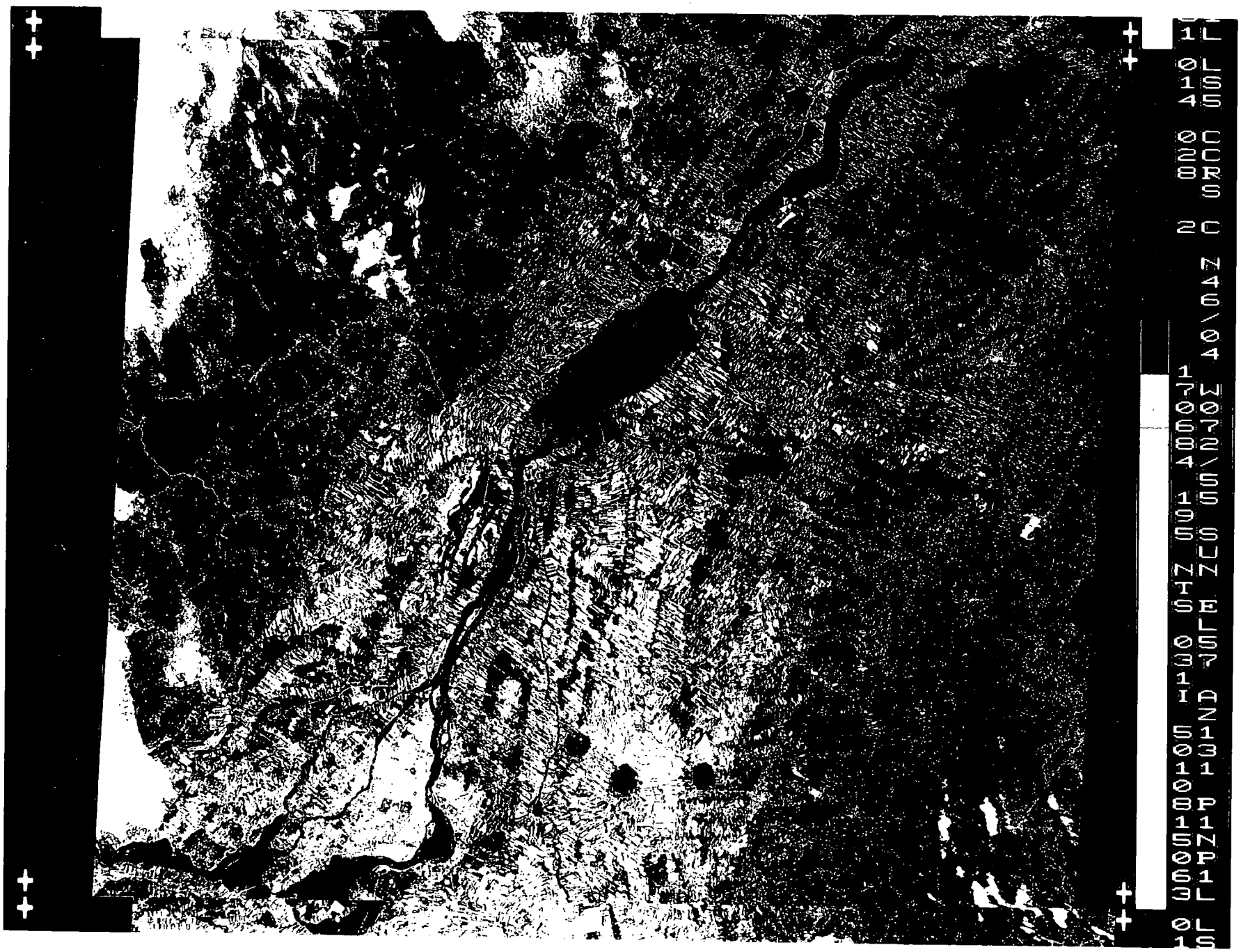

Figure 3

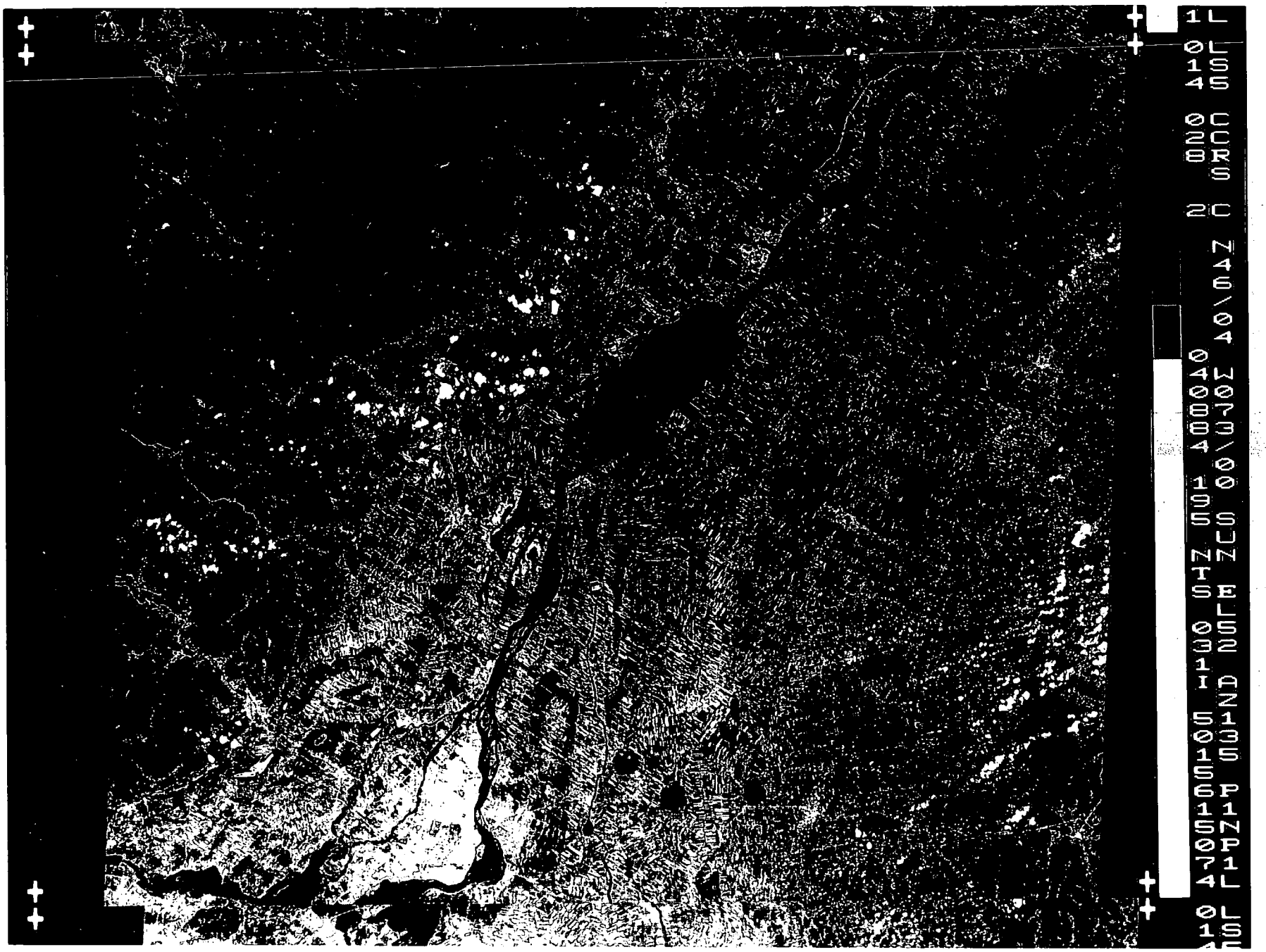

Figure 4

Figure 5

Figure 6

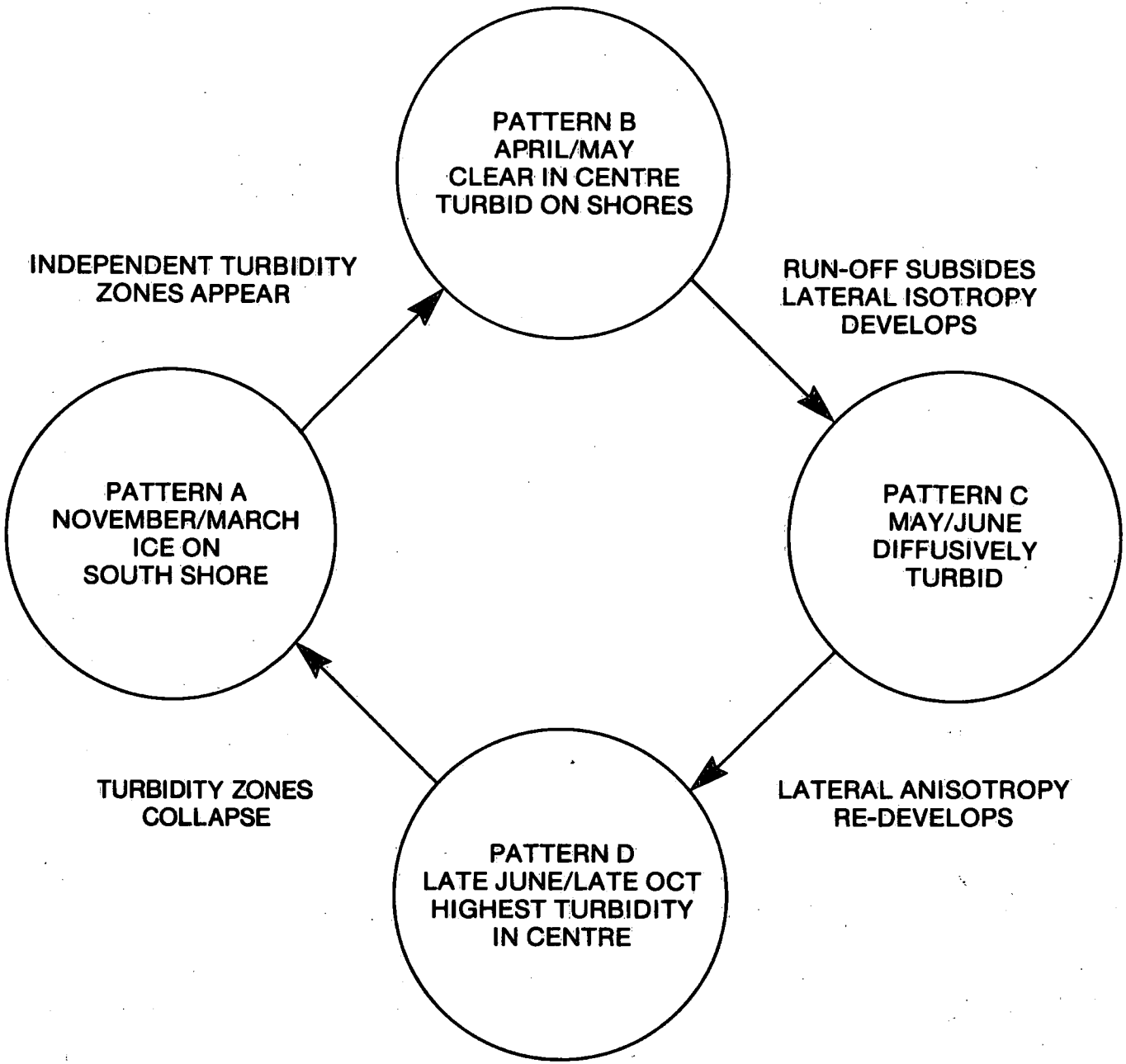
PATTERN B
APRIL/MAY
CLEAR IN CENTRE
TURBID ON SHORES
RUN-OFF SUBSIDES
LATERAL ISOTROPY
DEVELOPS
PATTERN C
MAY/JUNE
DIFFUSIVELY
TURBID
LATERAL ANISOTROPY
RE-DEVELOPS
PATTERN D
LATE JUNE/LATE OCT
HIGHEST TURBIDITY
IN CENTRE
TURBIDITY ZONES
COLLAPSE
PATTERN A
NOVEMBER/MARCH
ICE ON
SOUTH SHORE
INDEPENDENT TURBIDITY
ZONES APPEAR

Figure 7

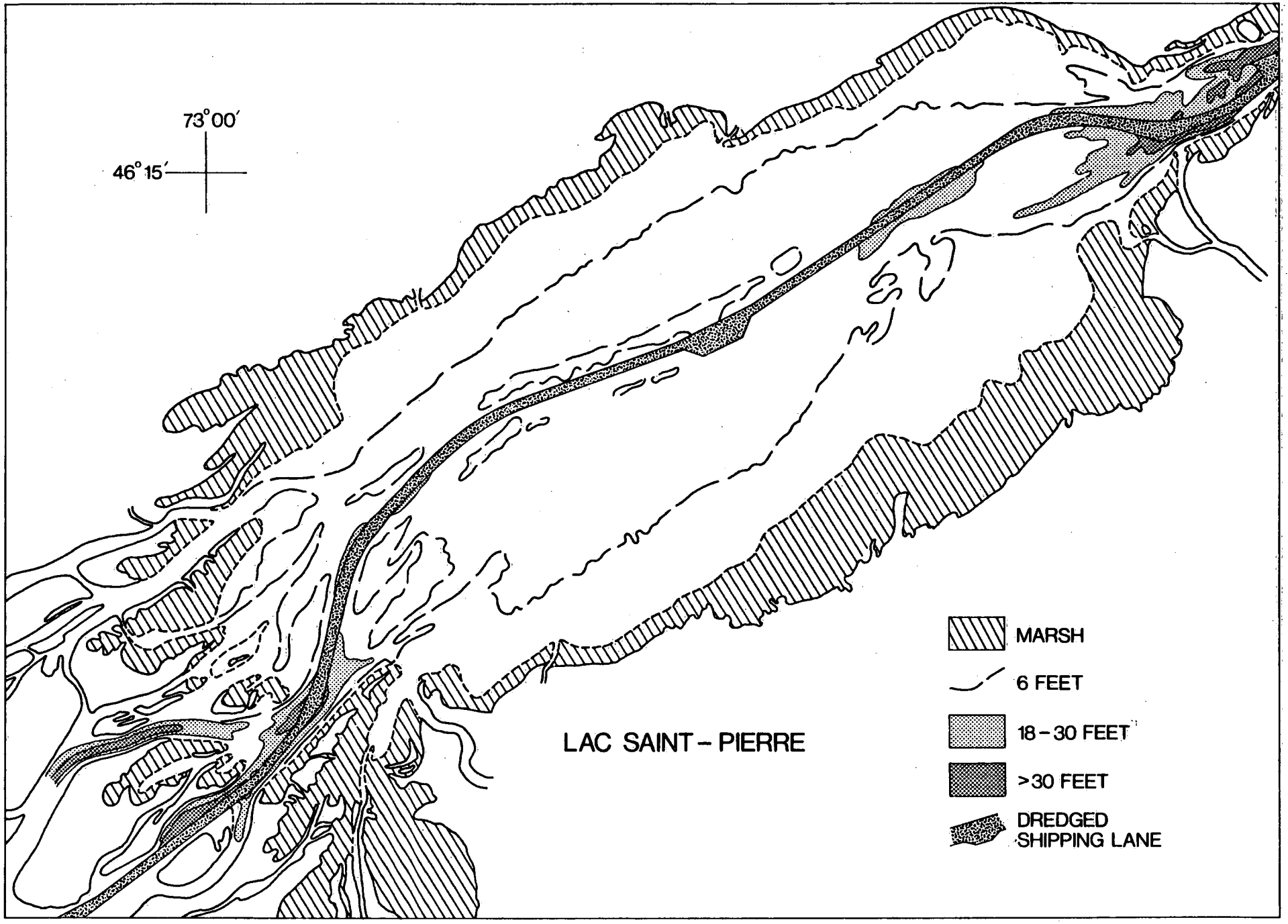
73°00′
46°15′
LAC SAINT-PIERRE
MARSH
6 FEET
18-30 FEET
>30 FEET
DREDGED
SHIPPING LANE

Figure 8

a

c

b

d

Plate 1

a

c

b

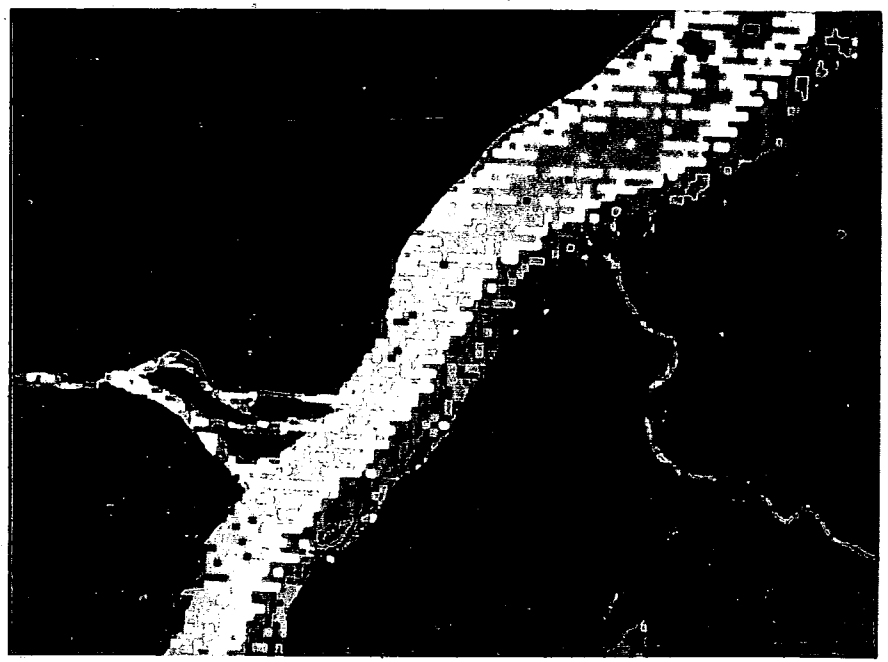

d

Plate 2